

## A Novel Topology of Zero-Current Transition (ZCT) Voltage-Source PWM three-phase Inverter

Dr. Mustafa M. Ibrahim  
Assistant Prof.

Basim Talib Kadhim  
Msc. student

Electrical Engineering Department  
College of Engineering – University of Basrah

### Abstract:

Soft-switching technique can substantially improve the performance of power converters, mainly due to the increase of switching frequency, that result in better modulation quality. This is more concerned particularly in the high power applications, where devices [gate turn off (GTO) or something else similar] can not operate over a few hundreds of hertz in conventional hard switching converter structures. High frequency resonant converter can perform the zero-current or zero-voltage switching (so, called soft switching) operation, which produces lower switching loss and lower EMI noise than the hard switching operation performed by conventional PWM converters.

In this paper, design and analysis of moderate power ZCT three-phase PWM inverter has been presented. Also, the designed inverter and its novel control circuit is implemented experimentally to investigate its characteristics with this new zero-current transition ZCT technique.

صنف جديد لتقنية الانتقال عند التيار الصفري (ZCT) لمغير ثلاثي الأطوار

### الخلاصة:-

إن أداء مغير القدرة عند الترددات العالية (حيث تستخدم الترددات العالية للحصول على تضمين الفضل) يمكن تحسينه باستخدام تقنية الغلق - الفتح الناعمة (soft-switching). إن تطبيق هذه التقنية يكون مهم عند القدرة العالية حيث لا تستطيع آلة الغلق - الفتح المستخدمة (مثل GTO وما يشابهها) العمل عند الترددات العالية أكبر من عدة مئات من الذبذبات /الثانية في حالة المغيرات التقليدية. مغيرات الرنين التي تعمل عند الترددات العالية بإمكانها أن تؤدي عملية الغلق - الفتح عند التيار الصفري أو الفولتية الصفيرية (ما يسمى بالغلق - الفتح الناعم) عند فقد قدرة قليل وضوضاء (EMI) قليلة مقارنة مع المغيرات تضمين عرض النبضة التقليدية (PWM).

تعرض هذه المقالة تصميم وتحليل لمغير ثلاثي الطور معكّل القدرة يعمل بتقنية الانتقال عند التيار الصفري، وقد تم التنفيذ المختبري للمغيرات المصممة ودوائر السيطرة عليها بقصد فحص خصائص هذه المغيرات التي تستخدم هذه التقنية الجديدة.

**Index Terms:** - DC-AC Inverter, Soft Switching and Zero Current Transition.

### 1- Introduction:-

High-performance inverters have always received the interest of considerable researchers. Due to many advantages of high efficiency, high operational frequency, small size and low switching stresses, soft switching topologies have brought the new trend to the industrial applications of next generation<sup>[1],[2],[3]</sup>

The development of zero switching loss inverter has attracted much interest for industrial applications. Utilizing the zero current transition ZCT technique in DC/AC inverter enables all main and auxiliary switches to be turned on and off under zero current conditions<sup>[1]</sup>. The zero current transition at both turn-on and turn-off not only reduces switching losses significantly but also eliminates the need for passive snubers<sup>[2]</sup>, due to the much reduced switch stress and cost.

A three-phase ZCT PWM voltage source inverter using auxiliary commutation is shown in Fig.1(a). The circuit operational waveforms for one switching cycle are illustrated in Fig.1(b), when the current of the main switch is reduced to zero prior to its turn-off. However, the turn-on loss of the main switch is not affected by the auxiliary circuit. The auxiliary switch turn-off current (at instant  $t_3$ ) is the same as the output current  $I_o$ , i.e., the same as the main switch turn-off current in the hard-switched converter. Therefore, this scheme is not suitable for high-power applications.

In this paper, new ZCT inverter schemes are proposed and analyzed to further improve the ZCT technique in Fig.1. With modified control and topology, all main switches and auxiliary switches are switched on and off under

zero-current conditions, so the switching losses and stresses are reduced significantly.

### 2- Analysis of the proposed ZCT three-phase inverter:

The drawbacks of ZCT topology shown in Fig.1 for the turn-on loss of the main switch is not affected by the auxiliary circuit and the peak voltage of resonant capacitor is about twice that of the switches. This voltage stress can be reduced by the topology shown in Fig.2(a). In this topology, two series-connected auxiliary switches are used for each leg with the low power diodes  $Dc_1$ - $Dc_6$  used to clamp the auxiliary switch voltage.

The operation of ZCT inverter presented here is characterized by soft switching<sup>[4]</sup> conditions which are achieved by actuating the auxiliary switching circuit in the transient periods.

The simulated waveforms during one switching period are shown in Fig.2(b). There are nine difference stages of the inverter circuit that can be discriminated during one switching period as illustrated in Fig.3.

On analyzing the inverter operation, the output current  $I_o$  is assumed constant during one commutating interval. Because of the symmetry of the circuit configuration, the consideration under the condition of the output current  $I_o > 0$  can be applied to case of  $I_o < 0$ . Before the main switch  $S_1$  turns on the output current  $I_o$  is conducted by  $D_2$ . The auxiliary current  $i_x$  is zero and the resonant capacitor voltage  $V_x$  has a value equal to  $V_{CO}$ . The nine inverter circuit stages are as follows.

**(a) Turn-On Transition I ( $t_0, t_1$ ):-**

At  $t_0$ ,  $S_{x1}$  is turned on initiating the turn-on transition. The auxiliary resonant tank consisting of  $L_x$  and  $C_x$  starts to resonate and the auxiliary current  $i_x$  resonates from zero to positive peak at  $t_1$ , while the current in the diode  $D_2$  is reduced to zero. So,  $S_1$  is turned on under ZCT condition at  $t_1$  and the turn-on loss is reduced significantly.

**(b) Turn-On Transition II ( $t_1, t_2$ ): -**

The current rises rate of the switch  $S_1$  after turn-on is limited by the resonant inductor. After  $t_1$ ,  $i_x$  decreases rapidly toward zero at  $t_2$  because the supply voltage  $V_s/2$  will oppose the flow of the resonant current.

**(c) Turn-On Transition III ( $t_2, t_3$ ):-**

At  $t_2$ ,  $i_x$  returns to zero. So the switch  $S_{x1}$  turns off at ZCT condition at  $t_2$ . Since the resonant capacitor voltages  $V_x$  is positive, then the auxiliary circuit continues resonating and negative  $i_x$  is conducted by the clamp diode  $Dc_2$ . This stage vanishes when the current  $i_x$  returns again to zero.

**(d) Switch-on Stage ( $t_3, t_4$ ):-**

When  $i_x$  returns to zero again at  $t_3$ ,  $Dc_2$  is turned off naturally. Then, the auxiliary circuit stops resonating and disconnected from the main circuit functionally. The converter resumes its PWM operation and the duration of this stage is determined by the PWM control.

**(e) Turn-off Transition I ( $t_4, t_5$ ):-**

Before the main Switch  $S_1$  is turned off, the auxiliary switch  $S_{x2}$  is turned on at  $t_4$ . The resonant tank starts to resonate again. The resonant path includes  $L_x$ ,  $C_x$  and the  $(V_s/2)$  input voltage. Current  $i_x$  is negative and its magnitude increases from zero to peak and then decreases. When  $i_x$  returns to zero at  $t_5$ ,  $S_{x2}$  is turned off under ZCT condition. Since the resonant capacitor voltages  $V_x$  is less than  $(-V_s/2)$  then switching on the auxiliary switch  $S_{x1}$  at  $t_5$  allows the auxiliary circuit to continue resonating after  $t_5$ . The positive  $i_x$  is conducted by  $S_{x1}$  and  $Dc_2$ . Hence the current of the main switch  $S_1$ ,  $(I_0 - i_x)$ , is decreasing for  $i_x$  increase. The interval of this stage is terminated at  $t_6$  when  $i_x$  reaches  $I_0$ .

**(f) Turn-off Transition II ( $t_6, t_7$ ):-**

At  $t_6$ ,  $i_x$  reaches  $I_0$  and the main switch current is reduced to zero. So, the switch  $S_1$  is turned off under the ZCT condition. As  $i_x$  keeps increasing after  $t_6$  the surplus current will flow through the parallel diode of  $S_1$  and clamp the voltage across  $S_1$  to zero. So, the gate signal of  $S_1$  can be removed without causing much turn off loss.

**(g) Turn-off Transition III ( $t_7, t_8$ ):-**

At  $t_7$ ,  $i_x$  falls to  $I_0$  and the parallel diode of  $S_1$  stops conducting. Hence the capacitor  $C_x$  recharges through the load at an approximately constant current of  $I_0$ . This mode end when the capacitor voltage becomes equals to  $(V_s/2)$  at  $t_8$  and tends to over charge due to the energy stored in inductor  $L_x$ .

(h) Turn-off Transition IV ( $t_8, t_9$ ):-

At  $t_8$ ,  $V_x$  is charged to  $(Vs/2)$  and the diode  $D_2$  starts conducting. So, the resonant tank begins to resonate again. As  $i_x$  resonates toward zero, the current in the main diode increases gradually and  $i_x$  returns to zero at  $t_9$  where  $S_{x1}$  is turned off at ZCT condition.

(i) Clamp diode on stage ( $t_9, t_{10}$ ):-

At  $t_9$ ,  $V_x$  is being charged to positive voltages above  $(Vs/2)$  and the clamp diode  $D_{c2}$  conducts the auxiliary current  $i_x$ . This current resonates from Zero to negative peak and returns back toward zero at  $t_{10}$ . At the end of this stage the resonant capacitor voltage  $V_x$  is equal  $V_{co}$  which is the same value as the initial voltage.

3- Design of the ZCT circuit: -

The design of the auxiliary circuit requires the determination of the capacitance  $C_x$  and inductance  $L_x$ . The auxiliary circuit should be designed to achieve zero current switching with maximum main current while keeping the power loss in the auxiliary circuit a minimum [5]. Since turn-off transition is more critical than the turn-on transition, the following design procedure is mainly based on the switch turn-off requirements. To reduce the switch loss, the duration of turn-off Transition [1],  $T_{off}=(t_7-t_6)$ , should be long enough such that most storage charge of the main switch will be recombined. In the following analysis the design is based on maximum output current  $I_o$ . From the state plane trajectory [6] of Fig.4 we can get.

$$T_{off} = t_7 - t_6 \quad \text{-----(1)}$$

$$T_{off} = 2(\cos^{-1} m)\sqrt{L_x C_x}$$

$$T_{off} = (T_o \cos^{-1} m) / \pi \quad \text{-----(2)}$$

$$\text{Where: } m = \frac{I_o}{I_{pk}}$$

$$T_o = 2\pi\sqrt{L_x C_x}$$

$I_{pk}$  is the resonant peak of  $i_x$  during turn-off. Assuming  $V_x$  is zero at  $t_4$  without losing much accuracy, we can estimate  $I_{pk}$  to be [11].

$$I_{pk} = \frac{Vs/2}{Z_o} \quad \text{Where:}$$

$$Z_o = \sqrt{\frac{L_x}{C_x}}$$

The value of  $T_{off}$  used in designing the resonant circuit depends on the switching devices. Generally  $T_{off}$  should be much longer than the current fall time of the main switch [7]. A longer  $T_{off}$  can be achieved by either increasing  $I_{pk}$  or increasing  $T_o$ . Our design objective is to minimize the conduction loss caused by the soft switching action for given  $T_{off}$ . From the state plane shown in Fig.4 we have:

$$\frac{1}{2}\omega_o T_{off} = \theta \quad \text{-----(3)}$$

and ;

$$\theta = \cos^{-1} \frac{I_o}{I_{pk}} = \cos^{-1} m \quad \text{-----(4)}$$

Using the above equations and definitions it can be shown that: -

$$\omega_o = \frac{1}{m} \frac{I_o}{C_x Vs/2} \quad \text{-----(5)}$$

Substituting for  $T_o$  using eq.(5) into eq.(2) yields:

$$T_{off} = 2mCx \frac{Vs/2}{I_o} \cos^{-1} m \quad \text{----(6)}$$

$$\text{Let } T_n = \frac{CxVs/2}{I_o} = \frac{Q}{I_o}$$

be the available turn-off time<sup>[8]</sup>, then:

$$T_{off} = 2mT_n \cos^{-1} m$$

$$T_{off} = 2\theta T_n \cos \theta \quad \text{----(7)}$$

The per unit turn-off time ( $T_{off}/T_n$ ) as a function of current ratio  $m$  is plotted in Fig.5. The optimum design condition is obtained at the maximum per unite turn-off time as shown in Fig.5. The criterion can be accurately calculated by setting the derivative of eq.(7) equal to zero and solving the resulting transcendental equation.

$$\frac{dT_{off}}{d\theta} = 2T_n (\cos \theta - \theta \sin \theta) = 0$$

$$\theta = \cot \theta \quad \text{----(8)}$$

By numerical solution of eq. (8) we get:

$$\theta = 0.86 \text{ rad} = 49.3^\circ$$

$$m = 0.652$$

Once  $m=M$  is chosen  $Lx$  and  $Cx$  can be calculated as follows:-

$$Lx = \frac{MT_{off} Vs}{4I_o \cos^{-1} M} \quad \text{----(9)}$$

$$Cx = \frac{I_o T_{off}}{MV_s \cos^{-1} M} \quad \text{----(10)}$$

A practical converter will have much more complex loss models for its component and the optimum design can only be achieved through experiment. The conduction duration of the auxiliary switch is always 75 % of the resonant cycle. The

main switch can be turned on or off around the resonant peak of  $i_x$ .

#### 4-Experimental Results: -

The three-phase ZCT inverter shown in Fig.6 has been built and tested. The control circuit of the main and auxiliary switches is illustrated in Fig.7. Also the synchronized pulses required to control the operation of the designed ZCT inverter are given in Fig.2. Load voltage of (50Hz) frequency has been obtained with switching frequency of (600Hz) and resonant frequency of (10KHz).

Power MOSFET's (type VN4000A) are used for all main and auxiliary switches. Figs.8-10, show the experimental waveforms. It can be seen that the circuit waveforms comply with theoretical on analysis and simulation. Fig.8 (a, b and c) shows the synchronized control pulses of the main switches and auxiliary switches. Fig.9(a) shows the output three-phase line-to-neutral voltages  $V_{an}, V_{bn}$  and  $V_{cn}$  for resistive load only. Fig.9(b and c) shows the output phase and line voltages respectively for resistive load. Whereas Fig.9(d and c) shows those voltages for inductive load. Fig.10 (a) shows the current of the main switch  $S_1$ . As it can be seen in this figure, the current is increasing at the beginning of the turn-off stage due to the resonant inductor current and then decreasing at the end of this stage to zero. The resonant capacitor voltage and inductor current waveforms are shown in Fig.10(b and c) respectively. It can be seen that waveforms are similar to those obtained from the theoretical analysis.

Fig.11 shows the measured efficiency of the implemented three-phase inverter for different values of the input

voltage. The efficiency has been calculated for the hard switching and soft switching conditions of the inverter. It can be seen that the measured efficiency of ZCT PWM inverter is higher than of the conventional PWM inverter at heavy load.

### 5-Conclusions: -

In this paper analysis of the steady-state operation of moderate power inverter has been presented and design algorithm to determine the components of the resonant tank has been developed.

The designed inverter has been implemented using power MOSFET switches and novel control circuit to produce a.c. power of (50HZ) frequency.

The theoretically depicted waveforms and these obtained experimentally are in good agreement, which means that switching loss and stress are reduced significantly.

The snubber can be reduced or eliminated in the ZCT inverter and its cost may be reduced while its efficiency, EMI emissions, reliability, and dynamic performance are improved. Experimental results prove that significant efficiency improvement can be achieved using the ZCT circuit.

### References: -

[1]- Hengchun Mao, Fred C. Y. Lee, xunwei zhou, Heping Dai, Mohammed Casun and Dushan Boroyerich. "Improved zero current transition converters for high power application," IEEE Trans. Ind. Applicat., Vol.33, No.5, pp.1220-1281, September/October 1997.

- [2]- Deepakray M. Divan. "The resonant dc link converter-a new concept in static power conversion," IEEE Trans. Ind. Applicat. Vol.25, No.2, pp.319-325, March/April 1989.
- [3]- Munçaki Ishida, Iitosh. Fujino, and Tukamas, Hori "Real time output voltage control method of quasi-ZCS series resonant HF linked dc-ac converter" IEEE Trans. On Power Electronics Vo.10, No.6, pp.776-783 November 1995.
- [4]- Carlos A. Canesion and Ivo. Barbi "Novel zero-current switching PWM converters," IEEE Trans. Ind. Applicat. Vol.44, No.3, pp.372-381, June 1997.
- [5]- Ahmed cheriti, Kamal Al-Haddad, Dessaint, A. Meynard and Din kar Mukhedkar "A rugged soft commutated PWM Inverter for ac drives," IEEE Trans. On Power Electronics Vo.7, No.2, pp.385-392, April 1992.
- [6]- Ramesh Oruganti and Fred. C. Lee "Resonant power processors part I-state plane analysis" IEEE Trans. Ind. Applicat. Vol.IA.21, No.6, pp.1453-1460, November/ December 1985.
- [7]- Jung. Goocho, Chang-Yong Jeong and Fred C. Lee "Zero voltage and zero-current-switching full-bridge PWM converter using secondary active clamp," IEEE Trans. On Power Electronics Vol.13, No.4, pp.601-607 July, 1998.
- [8]- William McMurray "Thyristor commutation in dc choppers a comparative study," IEEE Trans. Ind. Applicat. Vol.IA.14, No.6, pp.547-558, November/ December 1978.

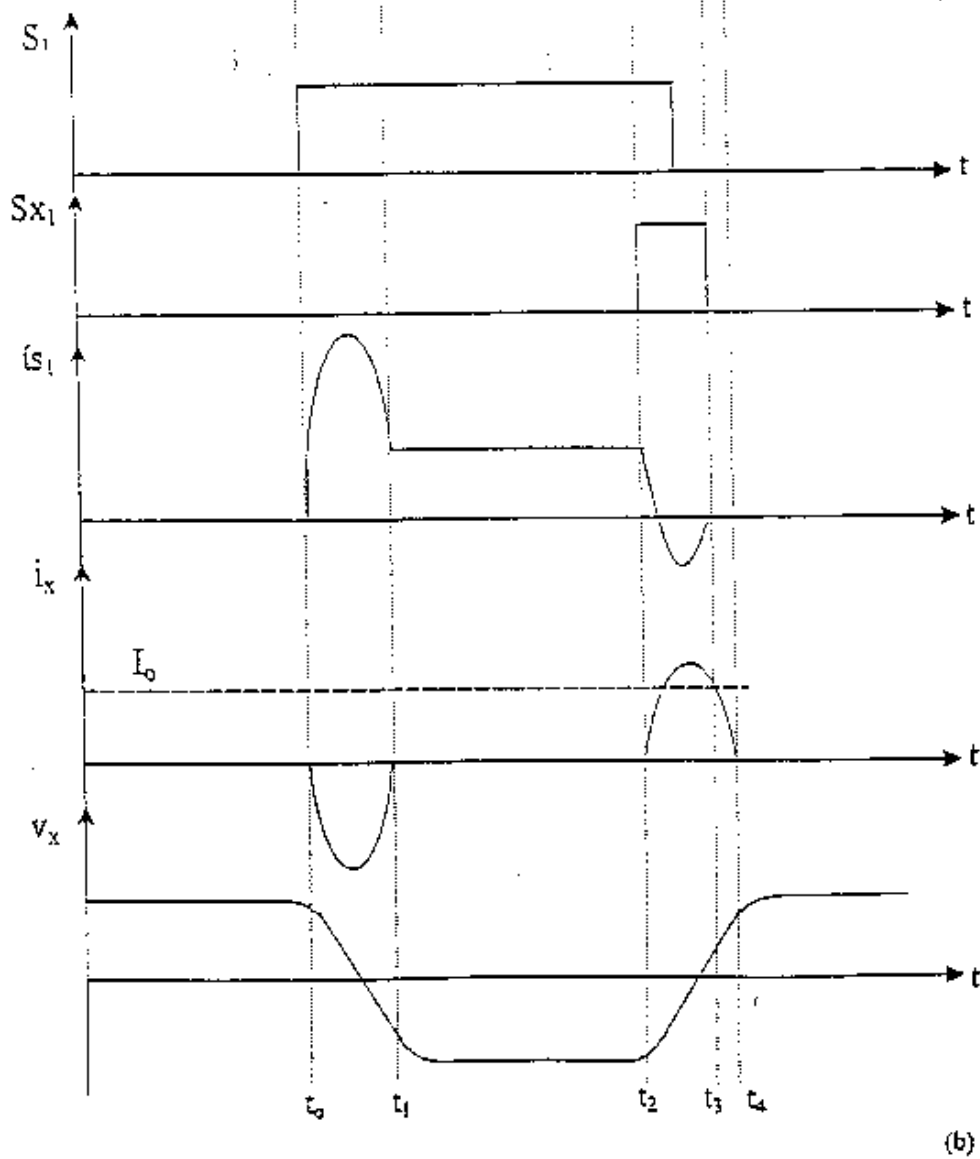
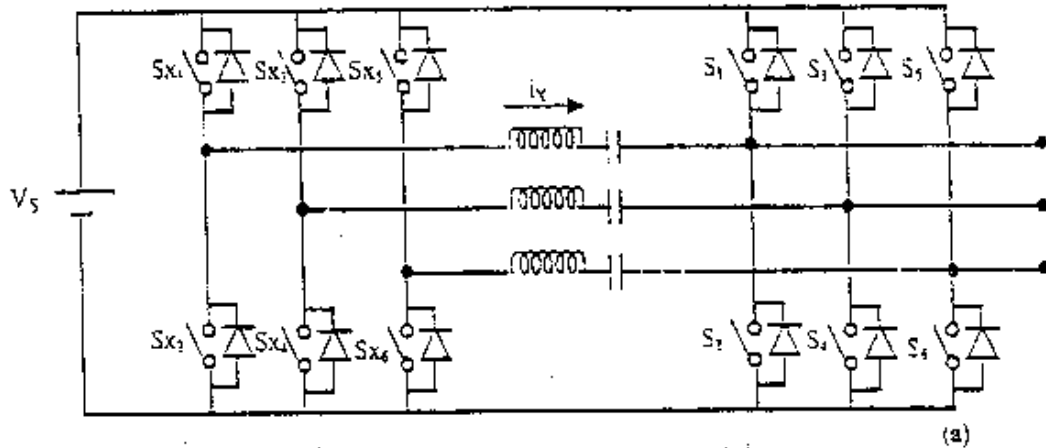
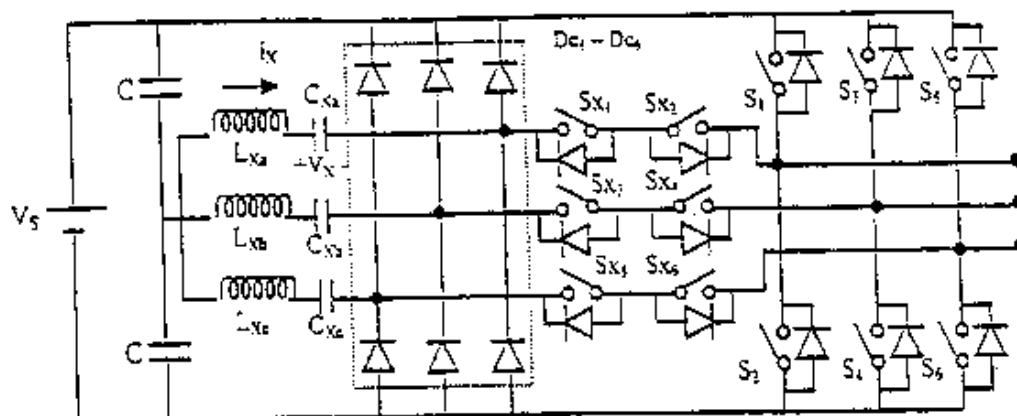


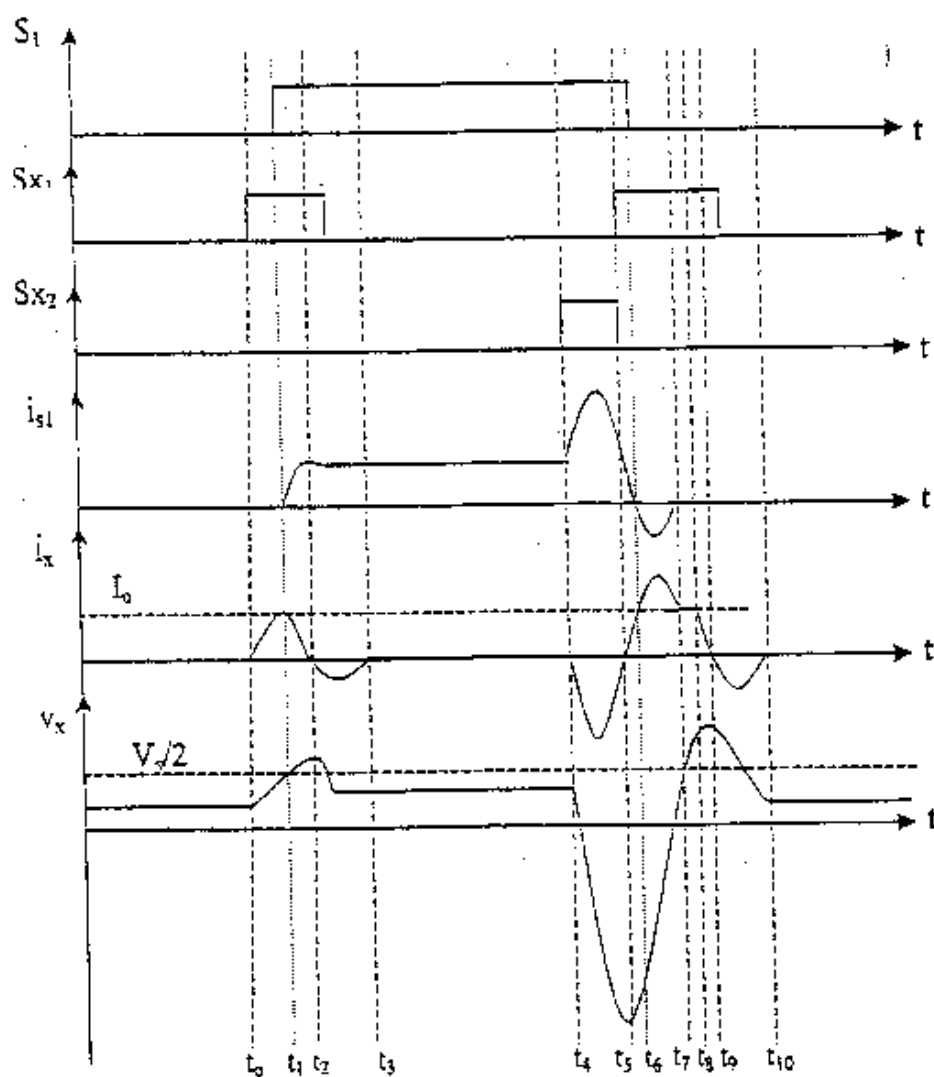
**Fig.1 :-Three-phase ZCT PWM inverter.**

(a) Topology.

(b) Operational waveforms in one switching cycle of  $S_1$ .



(a)



(b)

Fig.2:- New ZCT three - phase inverter.

(a) Topology.

(b) Operational waveforms in one switching cycle of  $S_{11}$ .



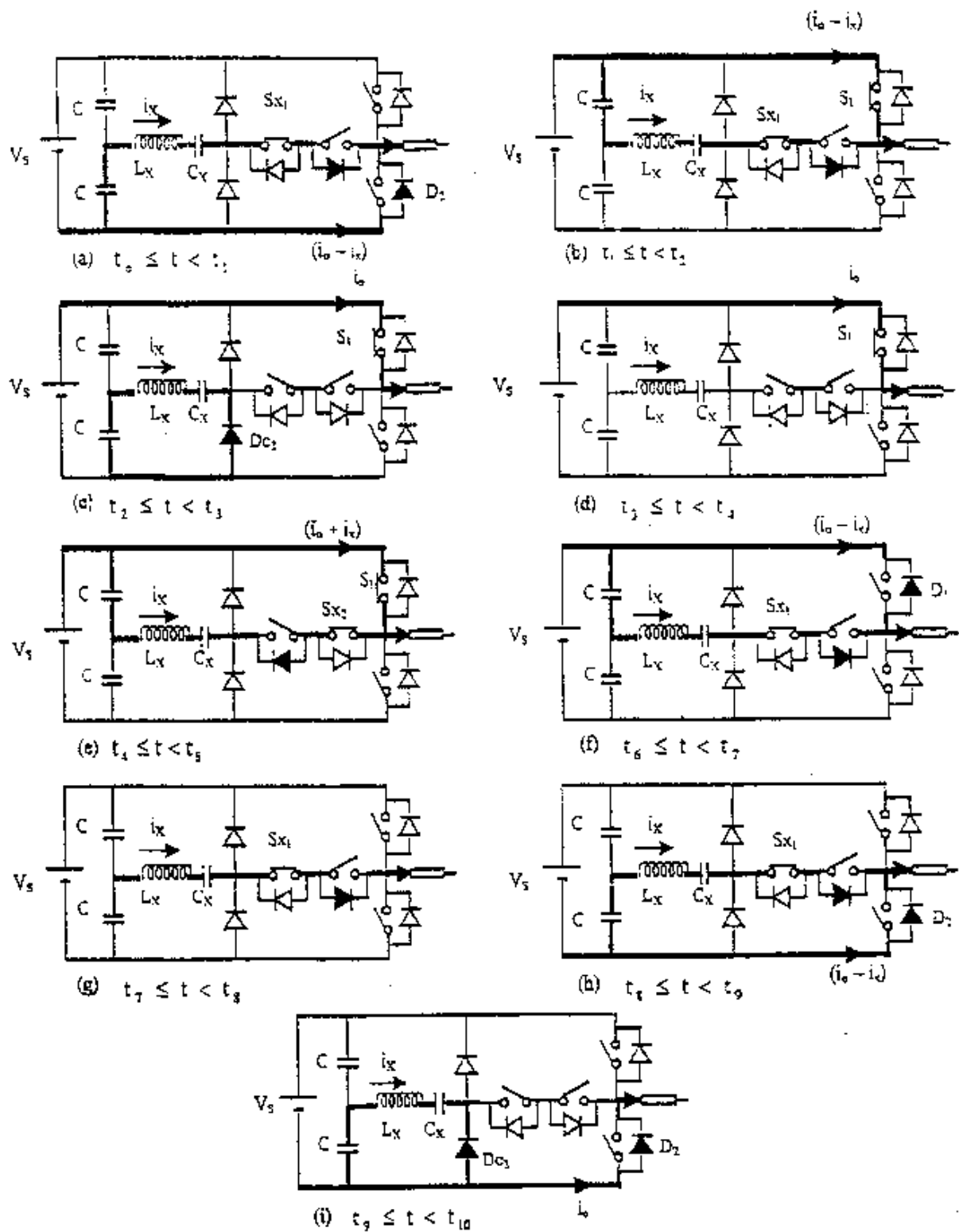


Fig.3 : - Operating stages in the soft - switching commutation.

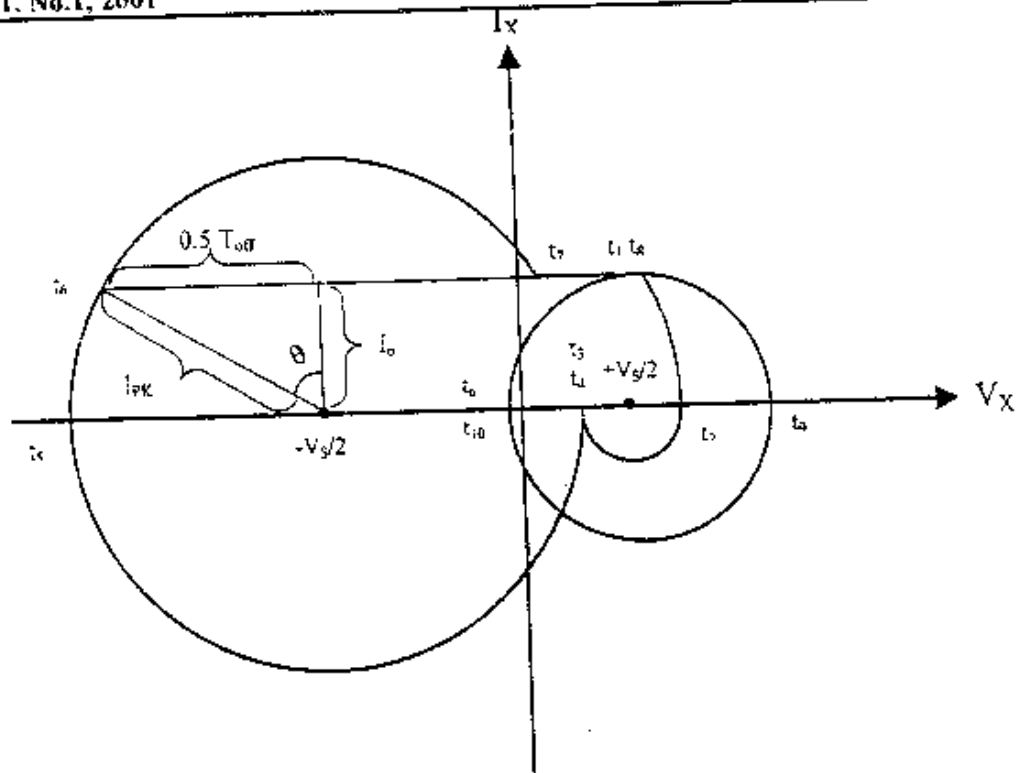


Fig.4 :- State plane trajectory

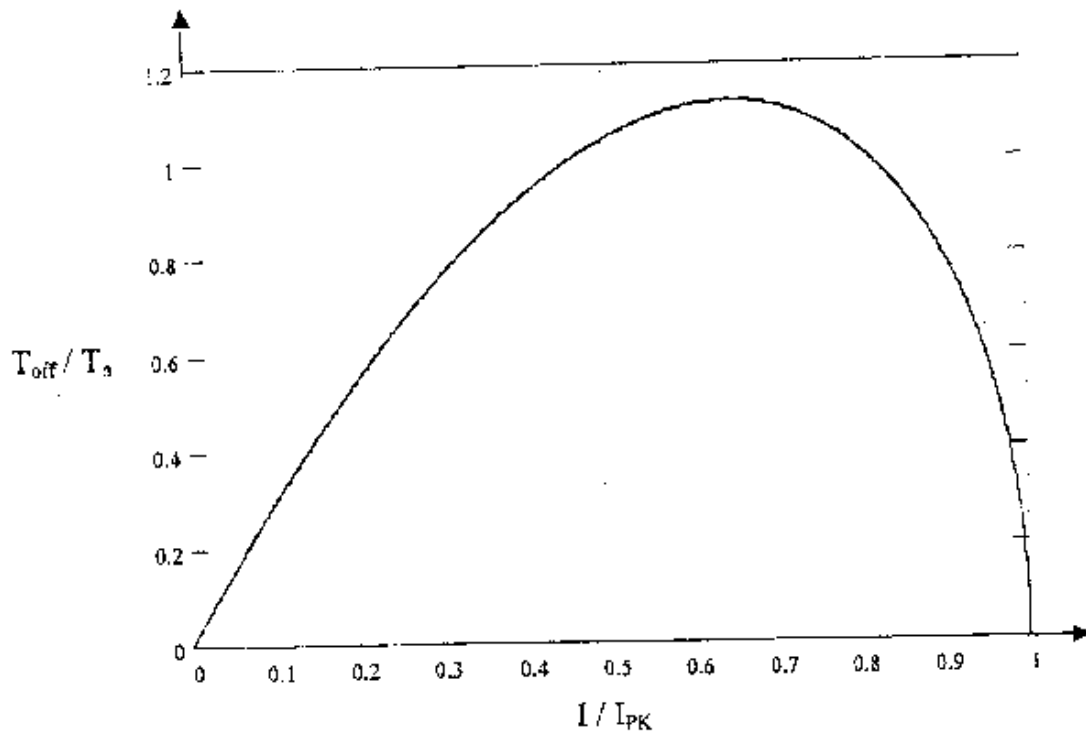


Fig.5 :- Turn off time in basic circuit as a function of current ratio parameter  $m$ .

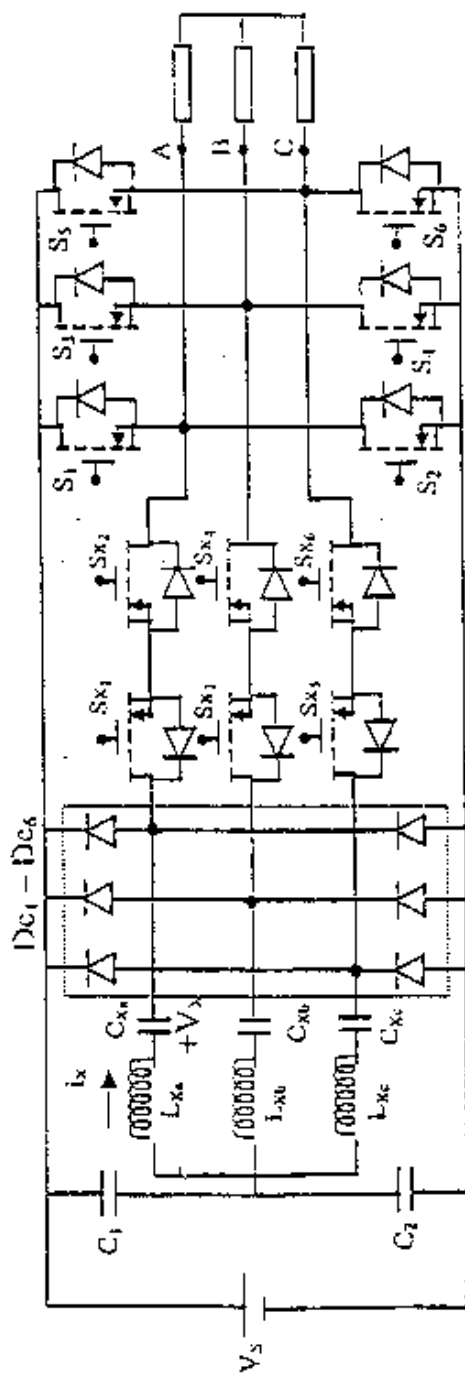


Fig.6 :- Three - phase ZCT inverter.

The implement:

$V_s = 50V$       $L_{xa} = L_{xb} = L_{xc} = 0.1297mH$  (Ferrite core )

$I_o = 2A$       $C_{xa} = C_{xb} = C_{xc} = 1.9526\mu F$  (Ceramic capacitance)

$C_1 = C_2 = 100 \mu F$

all diodes of the type BYX 71

all transistor of the type VN 4000A power MOSFET

Fig. 7:- Control circuit of three-phase ZCT inverter

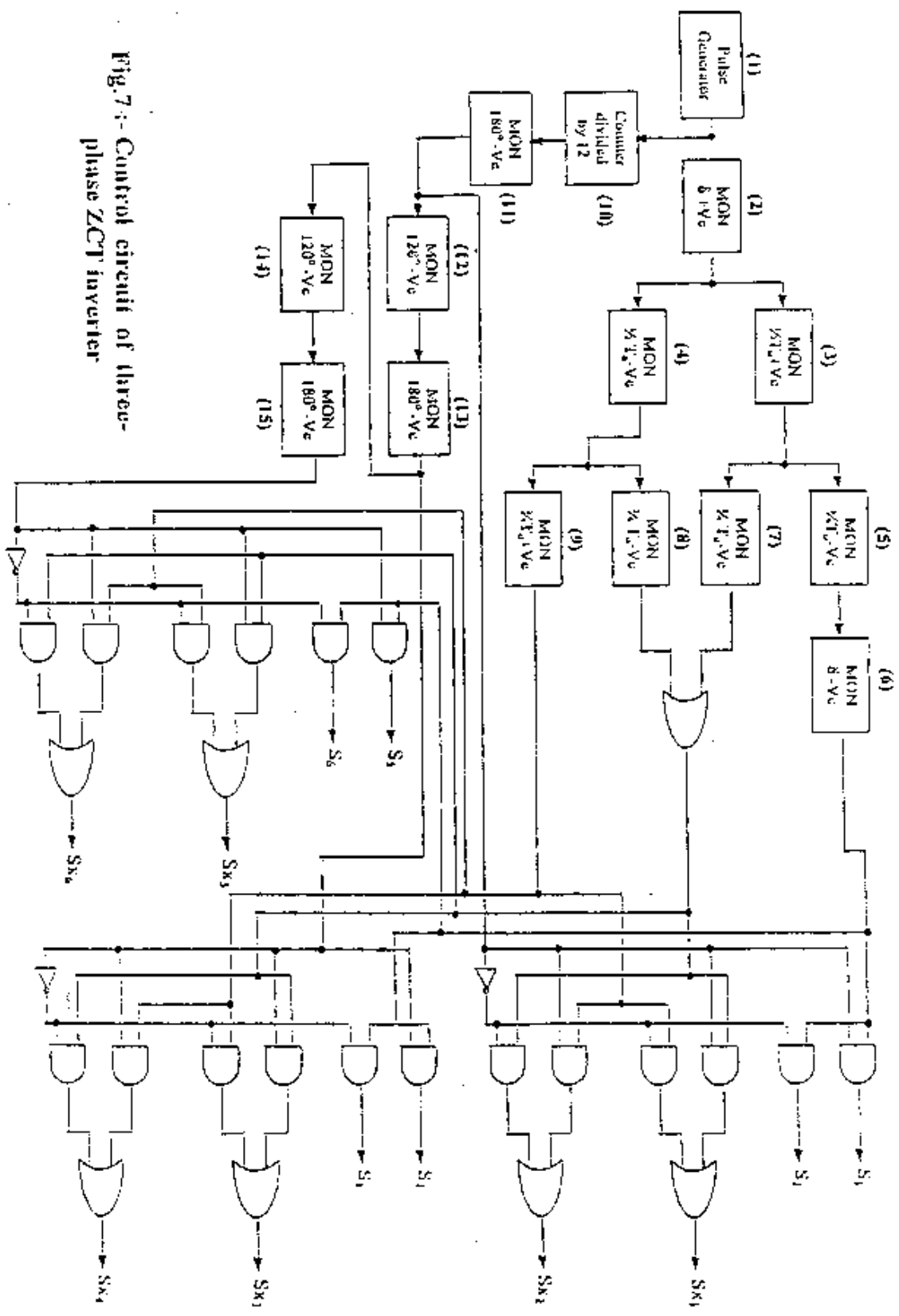
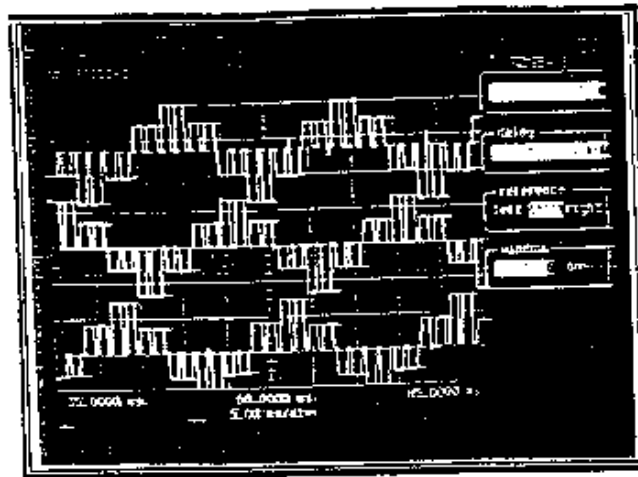
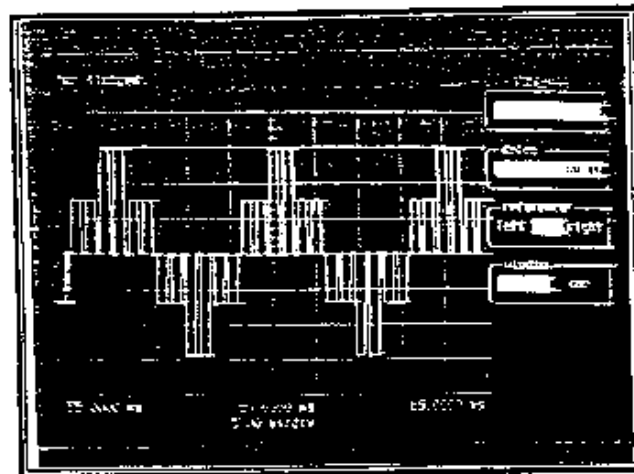


Fig.9 :-



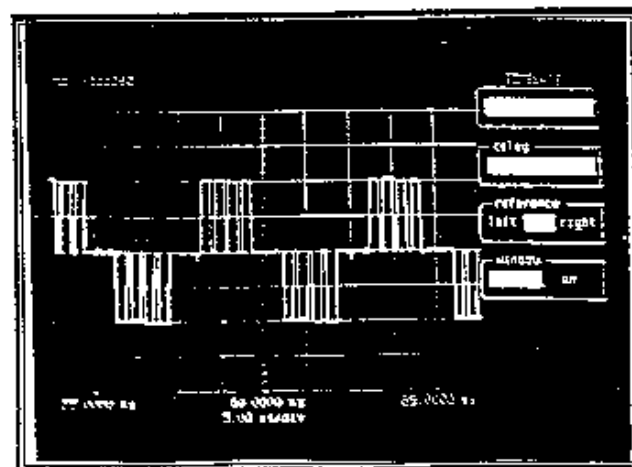
25 V/div  
 5 msec/div

a- output three-phase line-to-neutral voltages  $V_{an}$ ,  $V_{bn}$ , and  $V_{cn}$  at resistive load only .



10 V/div  
 5 msec/div

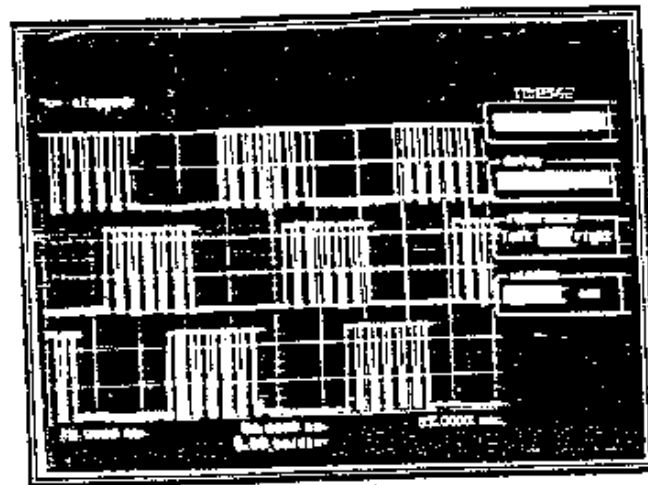
b- output line-to-neutral voltages  $V_{an}$  at resistive load only.



25 V/div  
 5 msec/div

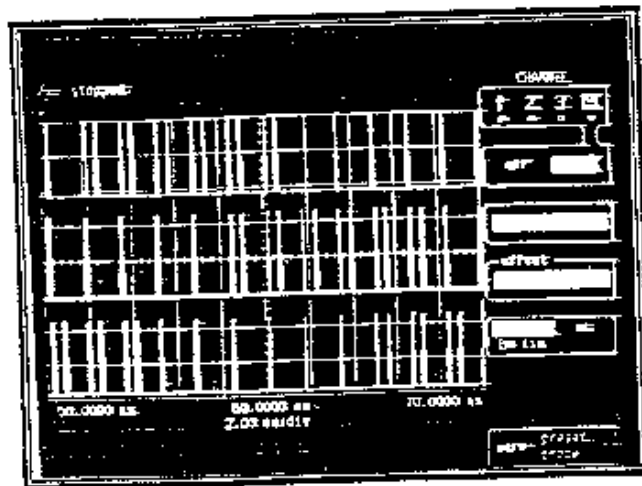
c- output line-to-line voltages  $V_{ab}$  at resistive load only.

Fig.3 :-



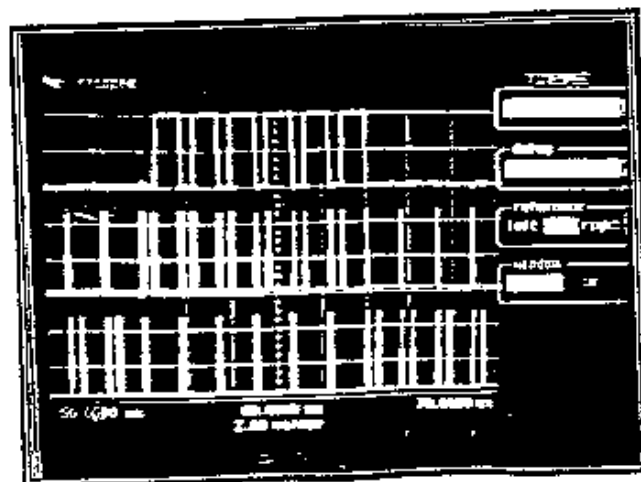
2 V/div  
5 msec/div

a- synchronized control pulse for  $S_1$ ,  $S_3$ , and  $S_5$



2 V/div  
2msec/div

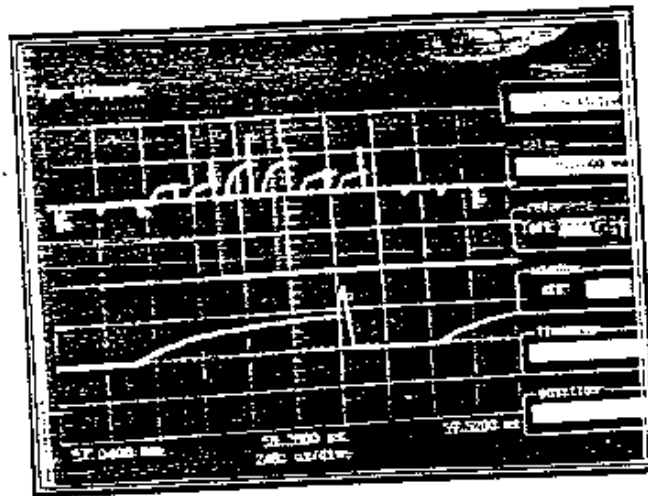
b- synchronized control pulse for  $S_{x1}$ ,  $S_{x3}$ , and  $S_{x5}$



2 V/div  
2 msec/div

c- synchronized control pulse for  $S_1$ ,  $S_{x1}$ , and  $S_{x2}$

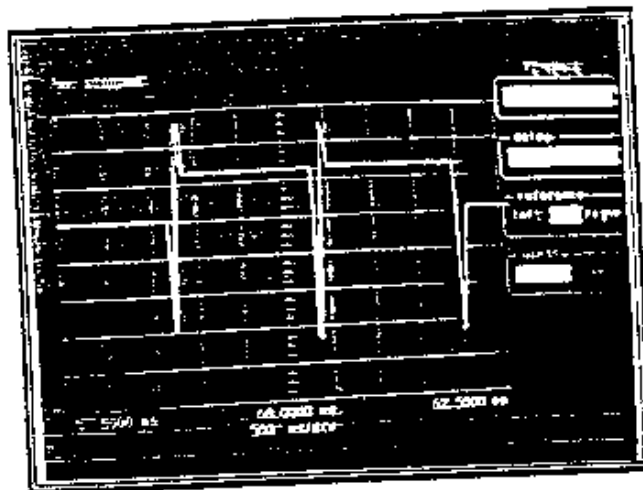
Fig.10 :-



Upper  
2 A/div  
2 msec/div

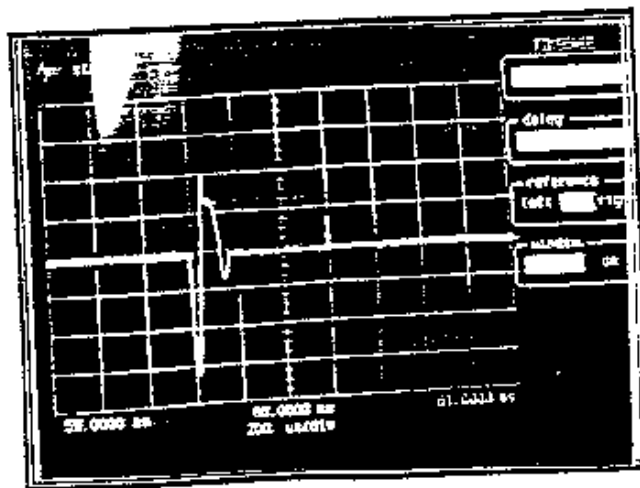
Lower  
2 A/div  
248  $\mu$ sec/div

a-  $i_{s1}$  current of switch  $S_1$ .



20 V/div  
500  $\mu$ sec/div

b- Resonant capacitor voltage  $V_{cr}$ .



2 A/div  
200  $\mu$ sec/div

c- Resonant inductor current  $i_{Lr}$ .

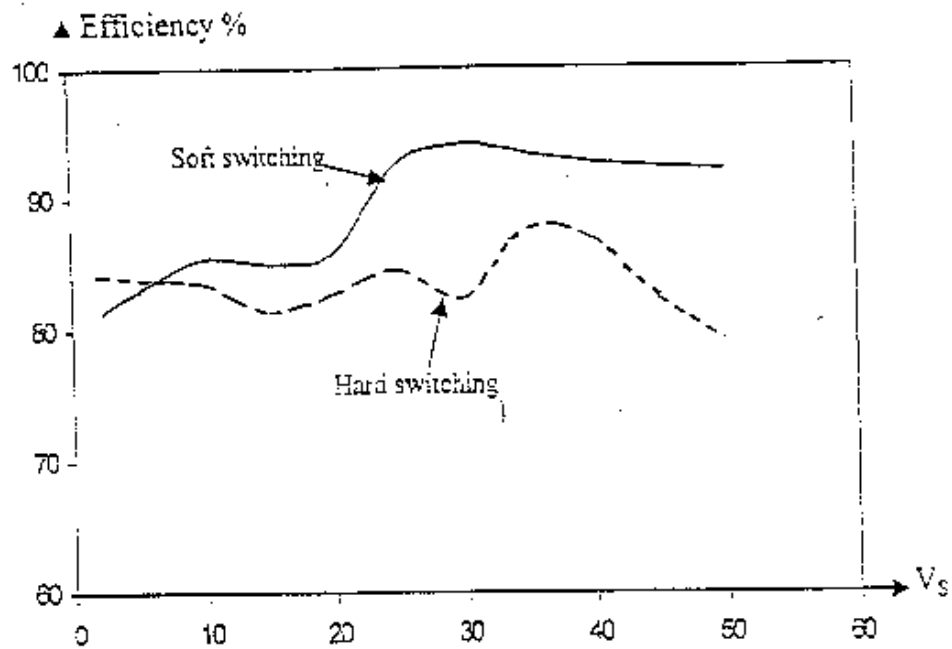


Fig.11 :- The change of the measured efficiency with input voltages at inductive load only for soft switching and hard switching three-phase inverter.